Structures 6 (2016) 99–106

Contents lists available at ScienceDirect

Structures

journal homepage: www.elsevier.com/locate/structures

Refined spatial beam-column element for second-order analysis of lattice shell structure

Lin Qi [a,*], Yang Ding [b]

[a] Airport College & Airport engineering research base, Civil Aviation University of China, Tianjin 300300, China
[b] School of Civil Engineering, Tianjin University, Tianjin 300072, China

ARTICLE INFO

Article history:
Received 7 January 2015
Received in revised form 30 January 2016
Accepted 1 February 2016
Available online 11 February 2016

Keywords:
Beam-column element
Second-order
Displacement interpolation function
Element tangent stiffness matrix
Lattice shell

ABSTRACT

Considering the coupling effect of axial force, bending moment and shear force, the displacement interpolation functions of the spatial beam-column element under axial tension and axial compression are derived respectively based on the differential equilibrium equations of the deformed member. The different displacement interpolation functions of the tension and compression elements are unified by replacing the stability integration functions with the Maclaurin series, and the unified functions are completely equivalent to those expressed by stability integration functions. The second-order element tangent stiffness matrix considering the effect of axial deformation, shear deformation, biaxial bending and torsion is derived. The number of series expansion terms in unified displacement interpolation functions is determined from aspects of calculation accuracy and positive definiteness of the structural general stiffness matrixes. Numerical calculation results by this element model accord well with the experimental data, and it indicates the accurateness of this element. Different element models are used in the analyses of a single layer lattice shell, and calculation results indicate that the geometrical nonlinearity of the structure is well exhibited with good efficiency by the refined spatial beam-column element proposed in this paper.

1. Introduction

There is additional bending moment in the member of lattice shell structure as it bears axial force as well as lateral force. So second order analysis is necessary, and the mechanical equilibrium equation should be constituted based on the deformed configuration of the member. Meek [1] and Chan [2] derived a geometrical stiffness matrix as the additional item of the stiffness matrix of the first-order Hermite element. This is a commonly used method to take the second order effect into account, but it is not so accurate by this method when one member is modeled by a single element (So and Chan [3]). Kondoh and Atluri [4] proposed a mixed beam element by which one member can be modeled by a single element, but the higher order terms of the displacement interpolation function are omitted. Chan and Zhou [5] proposed the pointwise equilibrating polynomial (PEP) element for nonlinear analysis of structure. It is a complex element model with a number of coefficients in the stiffness matrix compression, and the computational error gets larger in the case that the element carries quite big axial force when this model is used. Oran [6,7] element model is derived based on the deformed configuration of the member, and the element stiffness matrix is expressed by stability integration functions (Livesley and Chandler [8]). Though this model is applicable to the nonlinear analysis, it is not so accurate due to the omission of the shear effect and some coupling terms in the displacement interpolation functions of 3D element. Ekhande [9], Liew [10] and Zheng [11] proposed a refined spatial element model which is expressed by stability integration functions (SIFs) with the consideration of biaxial bending moment coupling effect. This is the analytical solution with a high accuracy. However, the displacement interpolation functions of the compression element are different from those of the tension element, and the calculation is relatively complicated. Chen [12], Goto [13] and Liew [14] used Taylor series to simplify the displacement interpolation functions of the spatial beam-column element, but the calculation result is markedly different in the case that the element carries quite small axial force. Li [15] proposed element stiffness matrix considering the effects of geometric nonlinearity, material nonlinearity and shear deformation. He also studied the influence of shear deformation on the beam element [16] and proposed a systemic analysis and design method of the steel frames [17]. Mohri et al. [18] developed a non-linear model that is performed in large torsion context according to a new kinematics that accounts for large torsion, flexural–torsional coupling and the presence of tapering terms in bending and torsion. Asgarian B et al. [19] investigated a numerical model based on the power series method for the lateral buckling stability of tapered thin-walled beams with arbitrary cross-sections and boundary conditions. Dourakopoulos et al. [20] developed a model for beams of arbitrary cross section considering the post-buckling effect and the moderate large displacements, large angles of

* Corresponding author.
E-mail address: qilin1208@163.com (L. Qi).

http://dx.doi.org/10.1016/j.istruc.2016.02.001
2352-0124/

twist and adopting second order approximations for the deflection–curvature relations. Couturier et al. [21] presented a method for analysis of the properties of general cross-sections with arbitrary geometry and material distribution. By this method the full six by six cross-section stiffness matrix is evaluated from a single element thickness slice represented by 3D solid elements with lengthwise Hermitian interpolation with six independent imposed deformation modes corresponding to extension, torsion, bending and shear. Hogsberg et al. [22] developed an element model for moderately thin-walled cross-sections. By this model the cubic interpolation is used to represent the quadratic shear stress variations along cross-section walls. Liu et al. [23,24] proposed a new and curved beam-column element with arbitrarily-located plastic hinge for second-order inelastic or direct analysis of steel frames. Li et al. [25] proposed a direct analysis method (DAM) for design of high-strength steel members and frames allowing explicit modeling of residual stresses. All the members of lattice shell structure bear the spatial external forces among which the axial force is markedly bigger in amount than the bending moment and shear force. So it is necessary to propose a refined element model for the lattice shell structure that is suitable to develop the computer program.

In this paper, the displacement interpolation functions of the spatial beam-column element under axial tension and axial compression are derived respectively based on the differential equilibrium equations of the deformed member with the consideration of the coupling effect of axial force, bending moment and shear force. The different displacement interpolation functions of the tension and compression elements are unified by replacing the stability integration functions with the Maclaurin series, and the unified functions are completely equivalent to those expressed by stability integration functions. The second-order element tangent stiffness matrix considering the effect of axial deformation, shear deformation, biaxial bending and torsion is derived. The number of Maclaurin series expansion terms in unified displacement interpolation functions is determined from aspects of calculation accuracy and positive definiteness of the structural general stiffness matrixes. For lattice shell structure the axial force, shear force and the bending moment are applied at the node. It is the end cross section of the structural member bears the maximum force. Under heavy load the end section of the structural member is considered to yield most likely, and the other sections maintain in linear. So the plastic hinge is arranged at the end section of the member, and the other segment is modeled by elastic element model which is proposed in this paper. The numerical analyses of the sample structures are then carried out to testify the precision and efficiency of the element.

2. Element displacement interpolation functions

The deformed planar beam-column element which bears compression axial force, bending moment and shear force is shown in Fig. 1.

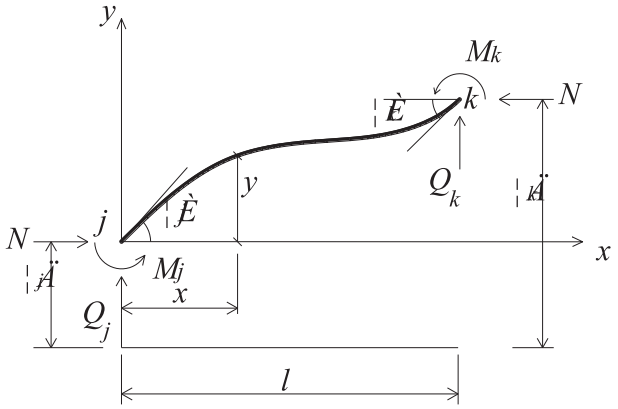

Fig. 1. Deformed planar beam-column element.

The axial force, bending moment and shear force are applied at the end section of the element. Based on the basic theory of material mechanics, the rotation of the element axis is assumed to be the shear strain at the element neutral axis. Based on Timoshenko theory about the element shear deformation, the rotation of the element cross section is independent with the lateral displacement. The curve of the element axis referable to the bending moment is calculated based on the plane cross-section assumption. The concentrate loads applied at the node do not turn with the rotation of the end section of the element.

The lateral deformation y at any cross section of a planar beam-column element consists of y_M caused by bending moment and y_Q caused by shear force. This is given by Eq. (1).

$$y = y_M + y_Q \tag{1}$$

Based on the plane cross-section assumption, the curve of the element axis referable to the bending moment is given by:

$$y''_M = -\frac{M}{EI} \tag{2}$$

where E is the elasticity modulus; I is the moment of inertia; M is the bending moment at any section of the element.

The mechanical equilibrium equation based on the deformed element which is shown in Fig. 1 is given by:

$$M = M_j - Q_j x + Ny \tag{3}$$

where N is the axial force of the planar beam-column element; M_j and Q_j are the bending moment and shear force at the element end j; x and y are shown in Fig. 1.

Based on the basic theory of material mechanics, the rotation of the element axis is assumed to be the shear strain at the element neutral axis. So the rotation of the element axis at any cross section referable to the shear force is given by:

$$y'_Q = \frac{\mu Q}{GA} = \frac{\mu}{GA}\cdot\frac{dM}{dx} \tag{4}$$

where G is the shear modulus; A is the cross section area; μ is the shape factor of the cross section.

Eq. (5) is constituted by substituting Eq. (3) in Eq. (4).

$$y'_Q = \frac{\mu Q}{GA} = \frac{\mu}{GA}\cdot\frac{dM}{dx} \tag{5}$$

Eq. (6) is derived by the derivation operation of Eq. (5).

$$y''_Q = \frac{\mu N}{GA}y'' \tag{6}$$

Eq. (5) is constituted by substituting Eq. (2) and Eq. (6) in the secondary derivative of Eq. (1).

$$y'' = -\frac{M}{EI} + \frac{\mu N}{GA}y'' = -\frac{M_j - Q_j x + Ny}{EI} + \frac{\mu N}{GA}y'' \tag{7}$$

Let $\eta = 1 - \mu N/(GA)$ and $\varpi^2 = N/(\eta EI)$. Eq. (8) is then constituted by substituting these two parameters in Eq. (7).

$$y'' + \varpi^2 y = -\frac{M_j - Q_j x}{\eta EI} \tag{8}$$

The general solution of Eq. (8) is given by Eq. (9).

$$y = a_1 \cos \varpi x + a_2 \sin \varpi x - \frac{M_j - Q_j x}{N} \tag{9}$$

where a_1 and a_2 are the undetermined coefficients.

The boundary conditions of the planar beam-column element shown in Fig.1 are given as follows: $y = 0$ and $y' = y'_M - y' = \theta_j + \mu(-Q_j + Ny')/GA$ when $x = 0$; $y = \delta_k - \delta_j$ and $y' = \theta_k - \mu(-Q_j + Ny')/GA$ when $x = l$ where l is the length of the element; δ_j and δ_k are the lateral displacements of the end j and end k; θ_k is the rotation of the end k.

The derivation above is based on the mechanical equilibrium equation of the deformed configuration of the planar beam-column element, so the second-order effect is taken into consideration. Substitute the boundary conditions in Eq. (9), and the lateral translational displacement interpolation function of the compression planar beam-column element can be acquired as the solution of this equation.

$$y = \frac{1}{\varphi_c}[\cos\varpi x(1-\cos\varpi l) - \sin\varpi l\sin\varpi x + \eta\varpi x\sin\varpi l - 1 + \cos\varpi l]\delta_j + \frac{1}{\varphi_c}[\sin\varpi l\sin\varpi x - \cos\varpi x(1-\cos\varpi l) - \eta\varpi x\sin\varpi x - \cos\varpi l + 1]\delta_k + \frac{1}{\eta\varpi\varphi_c}[\sin\varpi x(1-\cos\varpi l + \eta\varpi l\sin\varpi l) + \eta\varpi l\cos\varpi l - \sin\varpi l + \eta\varpi x\cdot(1-\cos\varpi l) + \cos\varpi x(\sin\varpi l - \eta\varpi l\cos\varpi l)]\theta_j + \frac{1}{\eta\varpi\varphi_c}[\sin\varpi l - \eta\varpi l + \sin\varpi x(\cos\varpi l - 1) + \cos\varpi x(\eta\varpi l - \sin\varpi l) + \eta\varpi x(1-\cos\varpi l)]\theta_k \tag{10}$$

where $\varphi_c = 2 - 2\cos\varpi l - \eta\varpi l\sin\varpi l$.

The shear force at the end j of the compression planar beam-column element can be acquired based on Eq. (10).

$$Q_j = \frac{EI\eta\varpi^2}{\varphi_c}\left[\eta\varpi\sin\varpi l(\delta_j - \delta_k) + (1-\cos\varpi l)(\theta_j + \theta_k)\right] \tag{11}$$

The shear force in the cross section with a distance of x away from the element end j is given by:

$$Q = -Q_j = -\frac{EI\eta\varpi^2}{\varphi_c}\left[\eta\varpi\sin\varpi l(\delta_j - \delta_k) + (1-\cos\varpi l)(\theta_j + \theta_k)\right] \tag{12}$$

Based on the Timoshenko [26] theory about the element shear deformation, the rotation of the element cross section is independent with the lateral displacement. So the rotation θ of the cross section with a distance of x away from the element end j is given by:

$$\theta = \frac{dy}{dx} - \frac{\mu Q}{GA} = \frac{dy}{dx} + \frac{\mu EI\eta\varpi^2}{GA\varphi_c}\left[\eta\varpi\sin\varpi l(\delta_j - \delta_k) + (1-\cos\varpi l)(\theta_j + \theta_k)\right] \tag{13}$$

The rotational displacement interpolation function of the compression planar beam-column element can be acquired by substituting Eq. (10) in Eq. (13).

$$\theta = \frac{\varpi}{\varphi_c}[\eta^2\sin\varpi l - \sin\varpi l\cos\varpi x - (1-\cos\varpi l)\sin\varpi x]\delta_j + \frac{\varpi}{\varphi_c}[\sin\varpi l\cos\varpi x + \sin\varpi x(1-\cos\varpi l) - \eta^2\sin\varpi l]\delta_k + \frac{1}{\eta\varphi_c}[\cos\varpi x(1-\cos\varpi l + \eta\varpi l\sin\varpi l) + \eta^2(1-\cos\varpi l) - \sin\varpi x(\sin\varpi l - \eta\varpi l\cos\alpha l)]\theta_j + \frac{1}{\eta\varphi_c}[\eta^2(1-\cos\varpi l) + \cos\varpi x(\cos\varpi l - 1) - \sin\varpi x(\eta\varpi l - \sin\varpi l)]\theta_k \tag{14}$$

Similarly, based on the differential equilibrium equations of the deformed member with tension axial force the lateral translational displacement interpolation function of the tension planar beam-column element with the consideration of the second-order effect can be derived as follows:

$$y = \frac{1}{\varphi_t}[\sh\varpi l\sh\varpi x - \eta\varpi x\sh\varpi l + \ch\varpi x(1-\ch\varpi l) + \ch\varpi l - 1]\delta_j + \frac{1}{\varphi_t}[\eta\varpi x\sh\varpi l - \sh\varpi l\sh\varpi x + \ch\varpi x(\ch\varpi l - 1) - \ch\varpi l + 1]\delta_k + \frac{1}{\eta\varpi\varphi_t}[\eta\varpi l\ch\alpha l - \sh\varpi l + \eta\varpi x\cdot(1-\ch\varpi l) + \sh\varpi x(1-\ch\varpi l + \eta\varpi l\sh\alpha l)\ch\varpi x(\sh\varpi l - \eta\varpi l\ch\varpi l)]\theta_j + \frac{1}{\eta\varpi\varphi_t}\cdot[(\ch\varpi l - 1)(\sh\varpi x - \eta\varpi) + \sh\varpi l - \eta\varpi l + \ch\varpi x(\eta\varpi l - \sh\varpi l)]\theta_k \tag{15}$$

where $\varphi_t = 2 - 2\ch\varpi l + \eta\varpi l\sh\varpi l$.

Similarly, based on the Timoshenko [26] theory about the element shear deformation, the rotation of the element cross section is independent with the lateral displacement. The rotational displacement interpolation function of the tension planar beam-column element with the consideration of the second-order effect is given by:

$$\theta = \frac{\varpi}{\varphi_t}[\sh\varpi x(1-\ch\varpi l) + \sh\varpi l\ch\varpi x - \eta^2\sh\varpi l]\delta_j + \frac{\varpi}{\varphi_t}[\eta^2\sh\varpi l - \sh\varpi l\ch\varpi x - \sh\varpi x(1-\ch\varpi l)]\delta_k + \frac{1}{\eta\varphi_t}[\sh\varpi x(\sh\varpi l - \eta\varpi l\ch\varpi l) + [\eta^2(1-\ch\varpi l) + \ch\varpi x(1-\ch\varpi l + \eta\varpi l\sh\varpi l)]\theta_j + \frac{1}{\eta\varphi_t}[(\ch\varpi l - 1)\cdot(\ch\varpi x - \eta^2) + \sh\varpi x(\eta\varpi l - \sh\varpi l)]\theta_k \tag{16}$$

According to Eq. (10), Eq. (14), Eq. (15) and Eq. (16), it is known that the expressions of the displacement interpolation functions of the compression element and the tension element are different. What shear with each other is that they are all constituted by stability integration functions such as sine, cosine, hyperbolic sine and hyperbolic cosine. The stability integration functions do not consist of variables by finite-time math operations such as addition, subtraction, multiplication, division, involution or evolution. Based on differential equilibrium equations of the deformed element the displacement interpolation functions with different expressions corresponding to the compression element and tension element are constituted by trigonometric function and hyperbolic function which are stability integration functions both. If the SIF formed displacement interpolation functions are used in the numerical calculation, the axial force needs to be checked at the beginning of each increment step. Moreover, in the numerical calculation the integration speed of stability integration functions is much slower than that of the polynomials. So it is less efficient when the SIF formed displacement interpolation functions are used in the numerical nonlinear calculation. In this paper, Maclaurin series are used to replace the stability integration functions, and the number of the expansion terms is determined from the aspects of calculation accuracy and positive definiteness of the structural general stiffness matrixes. Then the displacement interpolation functions are transformed into the polynomial form of a unified expression. The stability integration functions can be replaced by Maclaurin series as follows:

$$\sin\varpi l = \varpi l\left\{1 + \sum_{n=1}^{\infty}\frac{(-1)^n}{(2n+1)!}\left[(\varpi l)^2\right]^n\right\} \tag{17}$$

$$\cos\varpi l = 1 + \sum_{n=1}^{\infty}\frac{(-1)^n}{(2n)!}\left[(\varpi l)^2\right]^n \tag{18}$$

$$\sh\varpi l = \varpi l\left\{1 + \sum_{n=1}^{\infty}\frac{1}{(2n+1)!}\left[(\varpi l)^2\right]^n\right\} \tag{19}$$

$$\ch\varpi l = 1 + \sum_{n=1}^{\infty}\frac{1}{(2n)!}\left[(\varpi l)^2\right]^n \tag{20}$$

where n is the number of the series expansion terms.

The unified lateral translational displacement interpolation function and rotational translational displacement interpolation function of the compression element and tension element can be acquired by substituting Eqs. (17)–(20) in Eqs. (14)–(16).

$$y = B_1\delta_j + B_2\theta_j + B_3\delta_k + B_4\delta_k \tag{21}$$

$$\theta(x) = B_5\delta_j + B_6\theta_j + B_7\delta_k + B_8\delta_k \tag{22}$$

where

$$B_1 = -\frac{1}{\varphi}\chi_o\cdot\psi_o + \frac{1}{\varphi}\rho\xi\left[1+\chi_j\right]\left[1+\psi_j\right] - \frac{\eta}{\varphi}\rho\xi\left[1+\chi_j\right] \tag{23a}$$

$$B_2 = -\frac{l\psi_o}{\eta\varphi}\left[\left(1+\chi_j\right) - \eta(1+\chi_o)\right] - \frac{x}{\eta\varphi}\left[\chi_{op} - \rho_0\eta\left(1+\chi_j\right)\right] \cdot\left(1+\psi_j\right) - \frac{x}{\varphi}\chi_o \tag{23b}$$

$$B_3 = \frac{1}{\varphi}\chi_o\psi_o - \frac{1}{\varphi}\rho\xi\left(1+\chi_j\right)\cdot\left(1+\psi_j\right) + \frac{\eta\rho\xi}{\varphi}\left(1+\chi_j\right) \tag{23c}$$

$$B_4 = \frac{l\psi_o}{\eta\varphi}\left[\eta - \left(1+\chi_j\right)\right] + \frac{x}{\eta\varphi}\chi_o\left(1+\psi_j\right) - \frac{x}{\varphi}\chi_o \tag{23d}$$

$$B_5 = -\frac{\rho\xi}{l\varphi}\chi_o\left(1+\psi_j\right) + \frac{\rho}{l\varphi}\left(1+\chi_j\right)\cdot(1+\psi_o) - \frac{\rho\eta^2}{l\varphi}\left(1+\chi_j\right) \tag{23e}$$

$$B_6 = -\frac{\rho\xi}{\eta\varphi}\left[\left(1+\chi_j\right) - \eta(1+\chi_o)\right]\cdot\left(1+\psi_j\right) + \frac{1}{\eta\varphi}\left[\frac{\eta\rho_0}{l^2}\left(1+\chi_j\right) - \chi_o\right]\cdot(1+\psi_o) - \frac{\eta}{\varphi}\chi_o \tag{23f}$$

$$B_7 = \frac{\rho\xi}{l\varphi}\chi_o\left(1+\psi_j\right) - \frac{\rho}{l\varphi}\left(1+\chi_j\right)\cdot(1+\psi_o) + \frac{\rho\eta^2}{l\varphi}\left(1+\chi_j\right) \tag{23g}$$

$$B_8 = -\frac{\rho\xi}{\eta\varphi}\left(1-\eta+\chi_j\right)\cdot\left(1+\psi_j\right) + \frac{1}{\eta\varphi}\chi_o(1+\psi_o) - \frac{\eta}{\varphi}\chi_o \tag{23h}$$

where $\rho = |N|l^2/\eta EI$; $\rho_0 = Nl^2/\eta EI$; $\chi_o = \sum_{n=1}^{\infty}\rho^n/(2n)!$; $\chi_j = \sum_{n=1}^{\infty}\rho^n/(2n+1)!$; $\psi_o = \sum_{n=1}^{\infty}(\rho\xi^2)^n/(2n)!$; $\psi_j = \sum_{n=1}^{\infty}(\rho\xi^2)^n/(2n+1)!$; $\varphi = 2 - 2(1+\chi_o) + \rho\eta(1+\chi_j)$; $\xi = x/l$.

The linear displacement interpolation function is used for the axial displacement of the beam-column element. Extending the displacement interpolation functions of the planar element to three-dimensional analysis, the displacement interpolation function matrix of the spatial beam-column element for the second-order calculation is given by:

$$\boldsymbol{u}_c = \boldsymbol{B}\boldsymbol{u}_0 = \begin{bmatrix} 1-\xi & 0 & 0 & 0 & 0 & 0 & \xi & 0 & 0 & 0 & 0 & 0 \\ 0 & B_1 & 0 & 0 & 0 & B_2 & 0 & B_3 & 0 & 0 & 0 & B_4 \\ 0 & 0 & B_1 & 0 & -B_2 & 0 & 0 & 0 & B_3 & 0 & -B_4 & 0 \\ 0 & 0 & 0 & 1-\xi & 0 & 0 & 0 & 0 & 0 & \xi & 0 & 0 \\ 0 & 0 & -B_5 & 0 & B_6 & 0 & 0 & 0 & -B_7 & 0 & N_8 & 0 \\ 0 & B_5 & 0 & 0 & 0 & B_6 & 0 & B_7 & 0 & 0 & 0 & B_8 \end{bmatrix}\boldsymbol{u}_0 = \begin{bmatrix} \boldsymbol{B}_{ux} \\ \boldsymbol{B}_{uy} \\ \boldsymbol{B}_{uz} \\ \boldsymbol{B}_{\theta x} \\ \boldsymbol{B}_{\theta y} \\ \boldsymbol{B}_{\theta z} \end{bmatrix}\boldsymbol{u}_0 \tag{24}$$

where $\boldsymbol{u}_0 = \{u_{xj0}\ u_{yj0}\ u_{zj0}\ \theta_{xj0}\ \theta_{yj0}\ \theta_{zj0}\ u_{xk0}\ u_{yk0}\ u_{zk0}\ \theta_{xk0}\ \theta_{yk0}\ \theta_{zk0}\}$ which is the centroid displacement of the end cross section of the element; $\boldsymbol{u}_c = \{u_{xc}\ u_{yc}\ u_{zc}\ \theta_{xc}\ \theta_{yc}\ \theta_{zc}\}$ which is the centroid displacement of any cross section of the element.

3. Element tangent stiffness matrix

The tangent stiffness matrix of the spatial beam-column is derived based on the virtual work principle. The mechanical equilibrium equation of the beam-column element at the given moment $t + \Delta t$ in the virtual work form is shown in Eq. (25):

$$\int_{tV} {}_t^{t+\Delta t}\boldsymbol{s}^T\delta_t^{t+\Delta t}\boldsymbol{\varepsilon}\,\mathrm{d}^tV = {}_t^{t+\Delta t}W \tag{25}$$

where ${}_t^{t+\Delta t}\boldsymbol{s}$ is the Piola–Kirchhoff stress tensor at the given moment $t + \Delta t$; $\delta_t^{t+\Delta t}\boldsymbol{\varepsilon}$ is the vector of the Green–Lagrangian strain increment from the moment t to the moment $t + \Delta t$; V is the integration space; ${}_t^{t+\Delta t}W$ is the virtual work did by the external force at the moment $t + \Delta t$, which is given by:

$${}_t^{t+\Delta t}W = \int_{tV} {}_t^{t+\Delta t}\boldsymbol{q}_V^T\delta\boldsymbol{U}d^tV + \int_{tS} {}_t^{t+\Delta t}\boldsymbol{q}_S^T\delta\boldsymbol{U}d^tS + {}_t^{t+\Delta t}\boldsymbol{F}^T\delta\boldsymbol{u}_0 \tag{26}$$

where ${}_t^{t+\Delta t}\boldsymbol{q}_V$, ${}_t^{t+\Delta t}\boldsymbol{q}_S$ and ${}_t^{t+\Delta t}\boldsymbol{F}$ are the body force, surface force and the nodal concentrate force respectively; S is the integration area.

The stress, strain and displacement at the moment $t + \Delta t$ in the increment forms are given as follows:

$${}_t^{t+\Delta t}\boldsymbol{s} = {}_t^t\boldsymbol{\sigma} + {}_t\boldsymbol{s} \tag{27a}$$

$${}_t^{t+\Delta t}\boldsymbol{\varepsilon} = {}_t^t\boldsymbol{\varepsilon} + {}_t\boldsymbol{\varepsilon} \tag{27b}$$

$${}_t^{t+\Delta t}\boldsymbol{u} = {}_t^t\boldsymbol{u} + {}_t\boldsymbol{u} \tag{27c}$$

where ${}_t^t\boldsymbol{\sigma}$, ${}_t^t\boldsymbol{\varepsilon}$ and ${}_t^t\boldsymbol{u}$ are the stress vector, strain vector and displacement vector at the time t respectively. ${}_t\boldsymbol{s}$, ${}_t\boldsymbol{\varepsilon}$ and ${}_t\boldsymbol{u}$ are the stress increment vector, strain increment vector and the displacement increment vector at the time t respectively. ${}_t^{t+\Delta t}\boldsymbol{s}$, ${}_t^{t+\Delta t}\boldsymbol{\varepsilon}$ and ${}_t^{t+\Delta t}\boldsymbol{u}$ are the stress vector, strain vector and displacement vector at the time $t + \Delta t$ respectively.

The relationship between the stress increment vector ${}_t\boldsymbol{s}$ and the strain increment vector ${}_t\boldsymbol{\varepsilon}$ is given as follows:

$${}_t\boldsymbol{s} = {}_t\boldsymbol{C}_t\boldsymbol{\varepsilon} \tag{28}$$

where ${}_t\boldsymbol{C}$ is the constitutive matrix which is given by ${}_t\boldsymbol{C} = \mathrm{diag}\{E, G, G\}$.

The Green–Lagrangian strain increment vector ${}_t\boldsymbol{\varepsilon}$ consists of the linear component ${}_t\boldsymbol{e}$ and the nonlinear component ${}_t\boldsymbol{\vartheta}$. This is given by Eq. (29).

$${}_t\boldsymbol{\varepsilon} = {}_t\boldsymbol{e} + {}_t\boldsymbol{\vartheta} \tag{29}$$

Eq. (30) is acquired by substituting Eq. (28) and Eq. (29) in Eq. (25).

$$\int_{tV} {}_t\boldsymbol{\varepsilon}^T{}_t\boldsymbol{C}_t\delta\boldsymbol{\varepsilon}\,\mathrm{d}^tV + \int_{tV} {}_t^t\boldsymbol{\sigma}^T{}_t\delta\boldsymbol{\vartheta}\,\mathrm{d}^tV = {}_t^{t+\Delta t}W - \int_{tV} {}_t^t\boldsymbol{\sigma}^T{}_t\delta\boldsymbol{e}\,\mathrm{d}^tV \tag{30}$$

Let ${}_t\boldsymbol{\varepsilon} \doteq {}_t\boldsymbol{e}$ and $\delta_t\boldsymbol{\varepsilon} = {}_t\delta\boldsymbol{e}$, and substitute them in Eq. (30).

$$\int_{tV} {}_t\boldsymbol{e}^T{}_t\boldsymbol{C}_t\delta\boldsymbol{e}\,\mathrm{d}^tV + \int_{tV} {}_t^t\boldsymbol{\sigma}^T{}_t\delta\boldsymbol{\vartheta}\,\mathrm{d}^tV = {}_t^{t+\Delta t}W - \int_{tV} {}_t^t\boldsymbol{\sigma}^T{}_t\delta\boldsymbol{e}\,\mathrm{d}^tV \tag{31}$$

Let the x-axis of the rectangular coordinate system parallel to the element axial direction, and the y-axis and z-axis of the rectangular coordinate system parallel to the two cross-section directions. ${}_t^t\sigma_{xx}$, ${}_t^t\sigma_{xy}$ and ${}_t^t\sigma_{xz}$ are the independent stress components, and ${}_te_{xx}$, ${}_te_{xy}$, ${}_te_{xz}$, ${}_t\vartheta_{xx}$, ${}_t\vartheta_{xy}$ and ${}_t\vartheta_{xz}$ are the independent linear and nonlinear strain

components. Eq. (32) is constituted by substituting the stress components, the strain components and the constitutive matrix in Eq. (31).

$$\begin{aligned}&\int_{{}_tV}\left(E_t e_{xx_t}\delta e_{xx}+4G_t e_{xy\,t}\delta e_{xy}+G_t e_{xz_t}\delta e_{xz}\right)\mathrm{d}^{\mathrm{t}}V\\&+\int_{{}_tV}\left({}_t^{\mathrm{t}}\sigma_{xx_t}\delta\vartheta_{xx}+2{}_t^{\mathrm{t}}\sigma_{xy\,t}\delta\vartheta_{xy}+2{}_t^{\mathrm{t}}\sigma_{xz_t}\delta\vartheta_{xz}\right)\mathrm{d}^{\mathrm{t}}V={}_t^{\mathrm{t}+\Delta\mathrm{t}}W\\&-\int_{{}_tV}\left({}_t^{\mathrm{t}}\sigma_{xx_t}\delta e_{xx}+2{}_t^{\mathrm{t}}\sigma_{xy\,t}\delta^{\mathrm{t}}e_{xy}+2{}_t^{\mathrm{t}}\sigma_{xz_t}\delta e_{xz}\right)\mathrm{d}^{\mathrm{t}}V\end{aligned}\tag{32}$$

Let Δu_x, Δu_y and Δu_z represent the translational displacement increments anywhere in the cross section that has a distance of x away from end j of the element. Based on the basic theory of elastic–plastic mechanics, the components of the Green–Lagrangian strain increments can be expressed as follows:

$${}_te_{xx}=\frac{\partial\Delta u_x}{\partial x}\tag{33a}$$

$${}_te_{xy}=\frac{1}{2}\left(\frac{\partial\Delta u_x}{\partial y}+\frac{\partial\Delta u_y}{\partial x}\right)\tag{33b}$$

$${}_te_{xz}=\frac{1}{2}\left(\frac{\partial\Delta u_x}{\partial z}+\frac{\partial\Delta u_z}{\partial x}\right)\tag{33c}$$

$${}_t\vartheta_{xx}=\frac{1}{2}\left(\frac{\partial\Delta u_x^2}{\partial x}+\frac{\partial\Delta u_y^2}{\partial x}+\frac{\partial\Delta u_z^2}{\partial x}\right)\tag{33d}$$

$${}_t\vartheta_{xy}=\frac{1}{2}\left(\frac{\partial\Delta u_x}{\partial x}\cdot\frac{\partial\Delta u_x}{\partial y}+\frac{\partial\Delta u_y}{\partial x}\cdot\frac{\partial\Delta u_y}{\partial y}+\frac{\partial\Delta u_z}{\partial x}\cdot\frac{\partial\Delta u_z}{\partial y}\right)\tag{33e}$$

$${}_t\vartheta_{xz}=\frac{1}{2}\left(\frac{\partial\Delta u_x}{\partial x}\cdot\frac{\partial\Delta u_x}{\partial z}+\frac{\partial\Delta u_z}{\partial x}\cdot\frac{\partial\Delta u_z}{\partial z}+\frac{\partial\Delta u_y}{\partial x}\cdot\frac{\partial\Delta u_y}{\partial z}\right)\tag{33f}$$

Let Δu_{xc}, Δu_{yc}, Δu_{zc},$\Delta\theta_x$, $\Delta\theta_y$ and $\Delta\theta_z$ represent the translational and rotational displacement increments at the centroid of the cross section with a distance of x away from end j of the element. Based on the equilibrium of section internal forces, the translational displacement increments anywhere in this cross section can be expressed as follows:

$$\Delta u_x=\Delta u_{xc}+z\Delta\theta_y-y\Delta\theta_z\tag{34a}$$

$$\Delta u_y=\Delta u_{yc}-z\Delta\theta_z\tag{34b}$$

$$\Delta u_z=\Delta u_{zc}+y\Delta\theta_x\tag{34c}$$

The Green–Lagrangian strain increments anywhere in the cross section that has a distance of x away from end j of the element can be expressed by the displacement increments at the centroid by substituting Eq. (34) in Eq. (33).

$${}_te_{xx}=\Delta u'_{xc}+z\Delta\theta'_y-y\Delta\theta'_z\tag{35a}$$

$${}_te_{xy}=\frac{1}{2}\left(-z\Delta\theta'_x+\Delta u'_{yc}-\Delta\theta_z\right)\tag{35b}$$

$${}_te_{xz}=\frac{1}{2}\left(y\Delta\theta'_x+\Delta u'_{zc}+\Delta\theta_y\right)\tag{35c}$$

$${}_t\vartheta_{xx}=\frac{1}{2}\left[\left(\Delta u'_{xc}+z\Delta\theta'_y-y\Delta u'_{zc}\right)^2+\left(\Delta u'_{yc}-z\Delta\theta'_x\right)^2+\left(\Delta u'_{zc}+y\Delta\theta'_x\right)^2\right]\tag{35d}$$

$${}_t\vartheta_{xy}=\frac{1}{2}\left[-\left(\Delta u'_{xc}+z\Delta\theta'_y-y\Delta u'_{zc}\right)\Delta\theta_z+\left(\Delta u'_{zc}+y\Delta\theta'_x\right)\Delta\theta_x\right]\tag{35e}$$

$${}_t\vartheta_{xz}=\frac{1}{2}\left[\left(\Delta u'_{xc}+z\Delta\theta'_y-y\Delta u'_{zc}\right)\Delta\theta_y-\left(\Delta u'_{yc}-z\Delta\theta'_x\right)\Delta\theta_x\right]\tag{35f}$$

The stresses can be expressed by the sectional forces of the element.

$${}_t^{\mathrm{t}}\sigma_{xx}=\frac{F_x}{A}+\frac{M_y z}{I_y}-\frac{M_z y}{I_z}\tag{36a}$$

$${}_t^{\mathrm{t}}\sigma_{xy}=\frac{F_y}{A}-\frac{M_x z}{J_x}\tag{36b}$$

$${}_t^{\mathrm{t}}\sigma_{xz}=\frac{F_z}{A}+\frac{M_x z}{J_x}\tag{36c}$$

where F_x, F_y and F_z are the axial force and the shear forces along the two cross-section axes of the element. M_x, M_y and M_z are the torsional moments and the bending moments about the two cross-section axes of the element. J_x, I_y and I_z are the polar moments of inertia and the inertia moments about the two cross-section axes of the element.

The virtual work equation of the spatial beam-column element in the increment form is constituted by substituting Eq. (35) and Eq. (36) in Eq. (32).

$$\begin{aligned}&\frac{1}{2}\int_0^l EA\delta\left(\Delta u'_{xc}\right)^2\mathrm{d}x+\frac{1}{2}\int_0^l EI_y\delta\left(\Delta\theta'_y\right)^2\mathrm{d}x+\frac{1}{2}\int_0^l\left(GJ_x+F_x i_o^2\right)\delta\left(\Delta\theta'_x\right)^2\mathrm{d}x\\&+\frac{1}{2}\int_0^l EI_z\delta\left(\Delta\theta'_z\right)^2\mathrm{d}x+\frac{1}{2}\int_0^l\left[GA\delta\left(\Delta u'_{yc}-\Delta\theta_z\right)^2+GA\delta\left(\Delta u'_{zo}+\Delta\theta_y\right)^2\right]\mathrm{d}x\\&+\frac{1}{2}\int_0^l F_x\delta\left[\left(\Delta u'_{yc}\right)^2+\left(\Delta u'_{zc}\right)^2\right]\mathrm{d}x+\int_0^l F_y\delta\cdot\left(-\Delta u'_{xc}\Delta\theta_z+\Delta u'_{zc}\Delta\theta_x\right)\mathrm{d}x\\&+\int_0^l F_z\cdot\delta\left(\Delta u'_{xc}\Delta\theta_y-\Delta u'_{yc}\Delta\theta_x\right)\mathrm{d}x-\int_0^l M_y\delta\Delta u'_{yc}\Delta\theta'_x\mathrm{d}x\\&-\int_0^l M_z\delta\Delta u'_{zc}\cdot\Delta\theta'\mathrm{d}x_x-\int_0^l M_z\delta\Delta u'_{zc}\Delta\theta'_x\mathrm{d}x+\int_0^l\left[M_x i_{yx}\delta\left(\Delta\theta'_y\Delta\theta_z\right)\right.\\&\left.-M_x i_{zx}\delta\left(\Delta\theta'_z\Delta\theta_y\right)\right]\mathrm{d}x={}_t^{\mathrm{t}+\Delta\mathrm{t}}W-{}_t^{\mathrm{t}}W_i\end{aligned}\tag{37}$$

where $i_0^2=(I_y+I_z)/A$; $i_y^2=I_y/A$; $i_z^2=I_z/A$; $i_{yx}=I_y/J_x$; ${}_t^{\mathrm{t}}W_i$ is the virtual work did by the internal forces within the time of t.

Eq. (38) is constituted by substituting Eq. (35) in Eq. (32).

$$\begin{aligned}{}_t^{\mathrm{t}}W_i=\int_0^l&\left[F_x\delta\left(\Delta u'_{xc}\right)+F_y\delta\left(\Delta u'_{yc}-\Delta\theta_z\right)+F_z\delta\left(\Delta u'_{zc}+\Delta\theta_y\right)\right.\\&\left.+M_y\delta\left(\Delta\theta'_y\right)+M_z\delta\left(\Delta\theta'_z\right)+M_x\delta\left(\Delta\theta'_x\right)\right]\mathrm{d}x\end{aligned}\tag{38}$$

The sectional forces in any cross section can be expressed by the concentrated forces at the end of the element.

$$F_x=F_{xk}\tag{39a}$$

$$F_y=-\frac{M_{zj}+M_{zk}}{l}\tag{39b}$$

$$F_z=\frac{M_{yj}+M_{yk}}{l}\tag{39c}$$

$$M_x=M_{xk}\tag{39d}$$

$$M_y=-M_{yj}\left(1-\frac{x}{l}\right)+M_{yk}\frac{x}{l}\tag{39e}$$

$$M_z=-M_{zj}\left(1-\frac{x}{l}\right)+M_{zk}\frac{x}{l}\tag{39f}$$

where M_{yj} and M_{zj} are the bending moments about the two cross-section axes at the end j of the element. F_{xk}, M_{xk}, M_{yk} and M_{zk} are axial forces, torsional moments and the bending moments about the two cross-section axes.

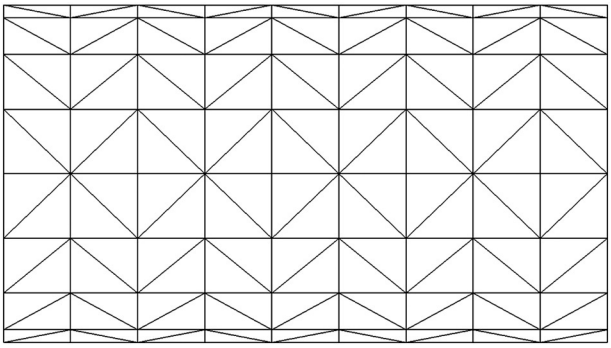

Fig. 2. The plan view of the cylindrical lattice shell.

Based on the virtual work principle, the tangent stiffness matrix of the spatial beam-column element is constituted by substituting Eq. (24) and Eq. (39) in Eq. (37).

$$\begin{aligned}\boldsymbol{K}_{\text{etc}} = {} & EA\boldsymbol{K}^{110}_{u_xu_x} + EI_y\boldsymbol{K}^{110}_{\theta_y\theta_y} + EI_z\boldsymbol{K}^{110}_{\theta_z\theta_z} + GJ_x\boldsymbol{K}^{110}_{\theta_x\theta_x} + F_{xk}\left(\boldsymbol{K}^{110}_{u_yu_y} + \boldsymbol{K}^{110}_{u_zu_z}\right) \\ & + F_{xk}i_0^2\boldsymbol{K}^{110}_{\theta_x\theta_x} + GA_y\cdot\left(\boldsymbol{K}^{110}_{u_yu_y} - \boldsymbol{K}^{010}_{\theta_zu_y} - \boldsymbol{K}^{100}_{u_y\theta_z} + \boldsymbol{K}^{000}_{\theta_z\theta_z}\right) \\ & + GA_z\left(\boldsymbol{K}^{110}_{u_zu_z} + \boldsymbol{K}^{010}_{\theta_yu_z} + \boldsymbol{K}^{100}_{u_z\theta_y} + \boldsymbol{K}^{000}_{\theta_y\theta_y}\right) + M_{xk}i_{yx}\cdot\left(\boldsymbol{K}^{100}_{\theta_y\theta_z} + \boldsymbol{K}^{010}_{\theta_z\theta_y}\right) \\ & - M_{xk}i_{zx}\left(\boldsymbol{K}^{100}_{\theta_z\theta_y} + \boldsymbol{K}^{010}_{\theta_y\theta_z}\right) + \frac{M_{yj}+M_{yk}}{l}\left(\boldsymbol{K}^{100}_{u_x\theta_y} + \boldsymbol{K}^{010}_{\theta_yu_x} - \boldsymbol{K}^{100}_{u_y\theta_x} - \boldsymbol{K}^{010}_{\theta_xu_y}\right. \\ & \left. - \boldsymbol{K}^{111}_{u_y\theta_x} - \boldsymbol{K}^{111}_{\theta_xu_y}\right) + M_{yj}\left(\boldsymbol{K}^{110}_{u_y\theta_x} + \boldsymbol{K}^{110}_{\theta_xu_y}\right) + \frac{M_{zj}+M_{zk}}{l}\left(\boldsymbol{K}^{100}_{u_x\theta_z} + \boldsymbol{K}^{010}_{\theta_zu_x}\right. \\ & \left. - \boldsymbol{K}^{100}_{u_z\theta_x} - \boldsymbol{K}^{010}_{\theta_xu_z} - \boldsymbol{K}^{111}_{u_z\theta_x} - \boldsymbol{K}^{111}_{\theta_xu_z}\right) + M_{zj}\left(\boldsymbol{K}^{110}_{u_z\theta_x} - \boldsymbol{K}^{110}_{\theta_xu_z}\right) \end{aligned} \tag{40}$$

where $\boldsymbol{K}^{b_1b_2b_3}_{b_4b_5} = \int_0^l \frac{\mathrm{d}^{b_1}\boldsymbol{B}_{b_4}}{\mathrm{d}x^{b_1}}^{\mathrm{T}} \cdot \frac{\mathrm{d}^{b_2}\boldsymbol{B}_{b_5}}{\mathrm{d}x^{b_2}} \cdot x^{b_3}\,\mathrm{d}x$ (41).

Where b_1 and b_2 are the numbers of the derivative order; x^{b_3} represents b_3^{th} power of x; b_4 and b_5 represent the displacements such as u_x, u_y, u_z, θ_x, θ_y and θ_z.

The effects of the axial deformation, shear deformation, biaxial bending and torsion are considered in Eq. (40). The element model proposed in this paper is mainly applicable for the members of lattice shell structure which bear the axial force of an amount much bigger than those of the bending moment and the shear force. Therefore, some coupling terms that play a less important role such as the self-coupling term of the shear force are omitted in the element tangent stiffness matrix.

4. Number of series expansion terms

Take a single layer cylindrical lattice shell as an example. The length and span of the structure are 27 m and 15 m. The structure bears a surface load of 1.2 kN/m^2, and the plan view is shown in Fig. 2. The SIF (Stability Integration Function) element model proposed in literatures [9–11] as well as the element model proposed in this paper are used for the structural analysis.

The displacement interpolation functions of SIF model are the analytical solutions of the mechanical equilibrium equation of the deformed member. It is a precise method although it is less efficient. When the series in Eq. (23a–h) are expanded by more terms, the result by the element of this paper gets closer to that of the SIF model, and it also accompanies a more calculation time. There will be an inflection point on the load–displacement curve when the general stiffness matrix of the structure gets non-positive. The inflection point usually corresponds to the ultimate bearing capacity of the structure. The element proposed in this paper with the expanded series by 4 terms to 10 terms is respectively used for the analyses of the example lattice shell, and the load proportion factors (LPFs) when the structural general stiffness matrix becomes non-positive are listed in Table 1. The numerical results of the vertical displacements of the structure central node by different elements are listed in Table. 2.

Table 1
LPFs when the general stiffness matrix becomes non-positive.

Element	SIF	10 terms	9 terms	8 terms	7 terms	6 terms	5 terms	4 terms
LPF	1.00	1.00	0.98	0.89	0.79	0.72	0.61	0.52

Table 2
Vertical displacements of the structure central node/mm.

LPF	Element							
	SIF	10 terms	9 terms	8 terms	7 terms	6 terms	5 terms	4 terms
0.1	13.23	13.23	13.23	13.23	13.23	13.20	13.23	13.23
0.2	25.82	25.82	25.82	25.82	25.82	25.82	25.82	25.82
0.3	38.84	38.84	38.84	38.84	38.84	38.84	38.84	38.84
0.4	52.51	52.51	52.51	52.51	52.51	52.51	52.51	52.42
0.5	66.88	66.88	66.88	66.88	66.88	66.88	66.83	65.92

From Table 2 it is known that there are only tiny differences between the calculation result by SIF element and those by element with the expanded series of 4 terms to 10 terms. When LPF is 0.5, the relative difference of the calculation results by SIF element and element proposed by this paper with the expanded series of 4 terms is only 1.43%. So from the point of view of precision, the series in the displacement interpolation function and the stiffness matrix need to be expanded by just 4 terms. However, it is also known from Table 1 that if the series are expanded by fewer terms, the structural general stiffness matrix gets non-positive at a small LPF. The more terms the series are expanded by, the bigger the LPF is when the stiffness matrix gets non-positive. The structural general stiffness matrix gets non-positive when LPF is 1.00 by SIF element as well as the element with the expanded series of 10 terms. So the series in the displacement interpolation functions and the stiffness matrix should be expanded by at least 10 terms.

5. Examples

5.1. Example 1

Gao [27] tested the deflections of a single layer spherical latticed shell model. The test model has a span of 3.6 m and the rise-span ratio of 1/7. The structure consists of circular steel bars of Φ14, and bears surface load of 4.0 kN/m^2. The plan view and the distribution of the survey points are shown in Fig. 3.

The calculation results by the element proposed by this paper and the test results of the deflections at the survey points are listed in

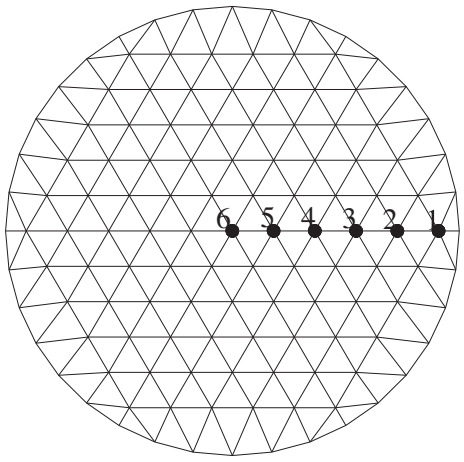

Fig. 3. Distribution of the survey points.

Table 3
Deflections at the survey points.

Survey points	1	2	3	4	5	6
Calculation results/mm	0.158	0.208	0.385	0.432	0.441	0.463
Test results/mm	0.165	0.218	0.382	0.451	0.443	0.436
Relative errors/%	−4.24	−4.59	0.79	−4.21	−0.45	6.19

Table 3. The curve of load proportion factor vs. displacement of Survey Point 5 is shown by Fig. 4.

From Table 3 and Fig. 4 it is known that the numerical results by the element proposed by this paper accord well with the test results. It indicates the precision of the element. The relative errors of the numerical results and the test results are all within 4.59% except for that of the Survey Point 6. It can be referable to the test error.

5.2. Example 2

Illustrated in Fig. 5, the cantilever beam 2.2 m long is constituted by steel section of $\Phi 114 \times 6$ (the cross-sectional diameter and thickness are 114 mm and 6 mm respectively). The cantilever beam which bears a changeless shear force of 3 kN and a variable axial compression force is simulated by a single element model proposed in this paper and a single general beam element B31, B32 and B33 of FEM program ABAQUS. The load increment method is used for the nonlinear analysis, and the vertical displacement at the end section is shown in Fig. 6.

It can be seen that there are two opposite trends in Fig. 6. When the model proposed in this paper is used for the cantilever beam that bears a changeless shear force, the bigger the axial force is, the larger the vertical displacement becomes. However the trend turns opposite when the general beam element models of ABAQUS are used. The second order effect that consists of P-Δ effect and P-δ effect is showing when the cantilever beam bears axial compression as well as the shear force. There is lateral displacement when the beam bears shear force, and the additional bending moment is then arose if it bears the axial force meanwhile. Therefore, the additional bending moment gets bigger along with the increment of axial compression force, and the vertical displacement at the end section of the beam will become greater consequently. Both of the P-δ effect caused by the member deformation and the P-Δ effect caused by the structure deformation should be taken into consideration in the second order analysis. P-Δ effect can be considered by nonlinear numerical solution methods such as load increment method, displacement increment method and arc length method. By these methods the structural equilibrium equations are formed based on the deformed structural configuration. P-δ effect is caused by the element deformation. In order to get a reasonable result, the higher order interpolation terms of the element model cannot be omitted when a structure member is modeled by a single element. In the general FEM program ABAQUS, B31 is the linear interpolation Timoshenko element,

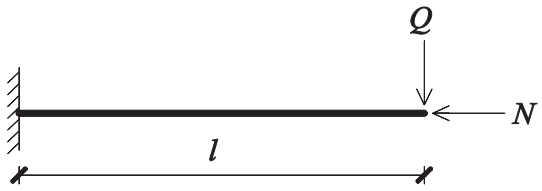

Fig. 5. The cantilever beam.

B32 is the interpolation quadratic Timoshenko element and B33 is the cubic interpolation Euler–Bernoulli element. The general FEM program pursues the balance between precision and efficiency of the calculation. Only the lower interpolation terms are considered in the beam element of the general FEM program. For the consideration of P-δ effect, usually more than one beam elements are used to model a member of bigger slenderness by this method, the P-δ effect is then transferred to P-Δ effect in the nonlinear solving process. However, there are no rules about how many elements are to be used for a member could contribute a precise result. A refined element should be of great applicability in the numerical analysis and well simulate the P-δ effect even the member is modeled just by a single element. The P-δ effect can be directly considered by the element model proposed in this paper and the P-δ effect does not need to be transferred to P-Δ effect if this element is used in the analysis. To verify the modeling of the second order effect by different element, the cantilever is modeled by a single element of different type in this example. Based on the accuracy and efficiency of the calculation, the higher order terms that have influence on the second order effect are all considered in the element model proposed in this paper. So it can be used to model the member by a single element.

5.3. Example 3

The element model proposed by this paper, Zheng [11] and Liew [14] are used respectively for the analyses of the cylindrical lattice shell shown in Fig. 2. The curve of the vertical displacement of the structure central node is shown in Fig. 7.

From Fig. 7 it can be seen that the calculation result by Liew [14] element is the smallest. When LPF is 0.96 the vertical displacements of the structure central node calculated by Liew [14] element is 31.80% smaller than that calculated by the element proposed in this paper. The coupling effect of the axial deformation and the shear deformation is not considered in the derivation of Liew [14] element. So the stiffness of the element is a little bit bigger. It has perceptible effect on the calculation result as the LPF increases. The arch effect, Wagner effect, the coupling effect of axial deformation and shear deformation, the coupling effect of axial force and torsion and the coupling effect of biaxial bending and torsion are all considered in Zheng [11] element. It is a complicated

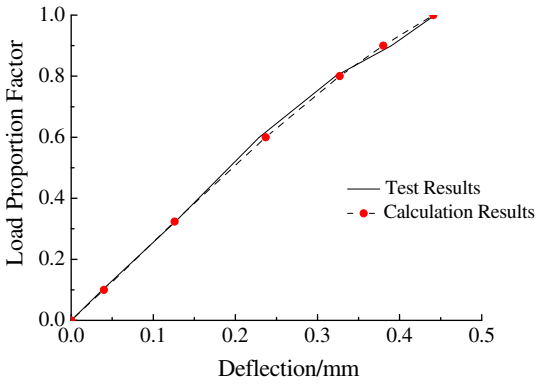

Fig. 4. The curve of load proportion factor vs. displacement of survey point 5.

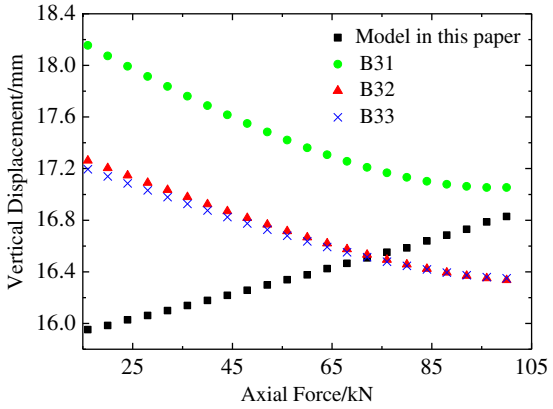

Fig. 6. Vertical displacement curve at the end section.

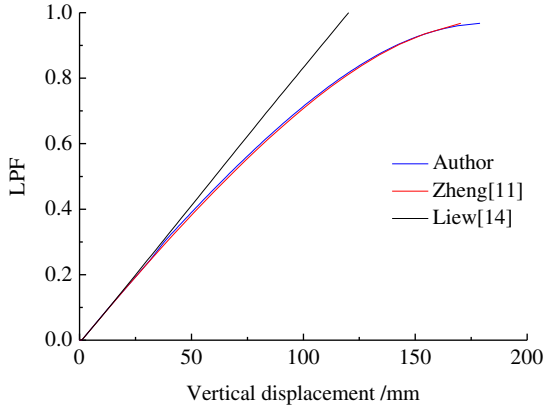

Fig. 7. Vertical displacements of the structure central node.

precise model though it is less efficient. The displacement curves calculated by the elements proposed by Zheng [11] in this paper are almost the same. The geometrical nonlinearity of the structure is well exhibited by these two curves which have a maximum relative difference of 1.68% only. It indicates the precision of the simplified element tangent stiffness matrix in the nonlinear analysis of lattice shells. Furthermore, the calculation efficiency is improved noticeably as a result of the simplification. The computation time of the analysis by Zheng [11] model is 25 times of that by element proposed in this paper. It indicates that the spatial beam-column element model proposed in this paper performs well in efficient.

6. Conclusions

(1) Considering the coupling effect of axial force, bending moment and shear force, the displacement interpolation functions of the spatial beam-column element under axial tension and axial compression are derived respectively based on the differential equilibrium equations of the deformed member.
(2) The different displacement interpolation functions of the tension and compression elements are unified by replacing the stability integration functions with the Maclaurin series, and the unified functions are completely equivalent to those expressed by stability integration functions. The number of series expansion terms in unified displacement interpolation functions is determined from aspects of calculation accuracy and positive definiteness of the structural general stiffness matrixes.
(3) The second-order element tangent stiffness matrix considering the effect of axial deformation, shear deformation, biaxial bending and torsion is derived.
(4) Numerical calculation results by this element model accord well with the experimental data, and it indicates the accurateness of this element. Different element models are used in the analyses of a single layer lattice shell, and calculation results indicate that the geometrical nonlinearity of the structure is efficiently exhibited by the refined spatial beam-column element proposed in this paper.

Acknowledgments

Financial supports from National Natural Science Foundation of China (51508557, 91315301), Open Fund of the Airport Engineering Research Base of Civil Aviation University of China (KFJJ2014JCGC05), Research Initial Fund of Civil Aviation University of China (2014QD08X), and Fundamental Research Funds for Central Universities "Seismic Isolation Control Research of Near-Fault Airport Architecture in High Seismic Intensity Region" are gratefully acknowledged.

References

[1] Meek JL, Tan HS. Geometrically nonlinear analysis of space frames by an incremental iterative technique. Comput Methods Appl Mech Eng 1984;47(3):261–82.
[2] Chan SL, Kitiporncai S. Geometric nonlinear analysis of asymmetric thin-walled beam-columns. Eng Struct 1987;9(4):243–54.
[3] So AKW, Chan SL. Buckling analysis of frames using 1 element/member[J]. J Constr Steel Res 1991;36(20):271–89.
[4] Kondoh K, Atluri SN. A simplified finite element method for large deformation, post-buckling analysis of large frame structures, using explicitly derived tangent stiffness matrices. Numer Methods Eng 1986;23(1):69–90.
[5] Chan SL, Zhou Z H. Pointwise equilibrating polynomial element for nonlinear analysis of frames. Struct Eng 1994;120(6):1703–17.
[6] Oran C. Tangent stiffness in plane frames. J Struct Div ASCE 1973;99(6):973–85.
[7] Oran C. Tangent stiffness in space frames. J Struct Div ASCE 1973;99(6):987–1001.
[8] Livesley RK, Chandler DB. Stability functions for structural frameworks. Manchester, England: Manchester University Press; 1956.
[9] Ekhande SG, Selvappalam M, Madugula MKS. Stability functions for three-dimensional beam-columns. Struct Eng 1989;115(2):467–79.
[10] Liew JYR, CHEN H, SHANMUGAM NE, et al. Improved nonlinear plastic hinge analysis of space frame structures[J]. Eng Struct 2000;22(10):1324–38.
[11] Zheng T, Zhao H. Modified dual nonlinear analysis of space steel frame structures[J]. Eng Struct 2003;20(6):202–8.
[12] Chen WF, Lui EM. Effects of joint flexibility on the behavior of steel frames. Comput Struct 1987;26(5):719–32.
[13] Goto Y, Chen WF. Second-order elastic analysis for frame design. J Struct Eng 1987;113(7):1501–19.
[14] Liew JYR, Punniyakotty NM, Shanmugam NE. Advanced analysis and design of spatial structures. J Constr Steel Res 1997;42(1):21–48.
[15] Guoqiang Li, Shen Zuyan. Unified matrix approach for nonlinear analysis of steel frames subjected to wind or earthquakes[J]. Comput Struct 1995;54(2):315–25.
[16] Guoqiang Li, Jinjun Li. Effects of shear deformation on the effective length of tapered columns with I-section for steel portal frames[J]. Struct Eng Mech 2000;20(5):479–89.
[17] Guoqiang Li, Jinjun Li. Advanced analysis and design of steel frames[M]. New Jersey, U. S.: John Wiley & Sons Inc.; 2007
[18] Mohri F, Meftah SA, Damil N. A large torsion beam finite element model for tapered thin-walled open cross sections beams[J]. Eng Struct 2015;99:132–48.
[19] Asgarian B, Soltani M, Mohri F. Lateral-torsional buckling of tapered thin-walled beams with arbitrary cross-sections[J]. Thin-Walled Struct 2012;62:96–108.
[20] Dourakopoulos JA, Sapountzakis EJ. Postbuckling analysis of beams of arbitrary cross section using BEM[J]. Eng Struct 2010;32(11):3713–24.
[21] Couturier PJ, Krenk S, Hogsberg J. Beam section stiffness properties using a single layer of 3D solid elements[J]. Comput Struct 2015;156:122–33.
[22] Hogsberg J, Krenk S. Analysis of moderately thin-walled beam cross-sections by cubic isoparametric elements[J]. Comput Struct 2014;134:88–101.
[23] Siwei Liu, Yaopeng Liu, Siulai Chan. Direct analysis by an arbitrarily-located-plastic-hinge element: part 1: planar analysis. J Constr Steel Res 2014;103:303–15.
[24] Siwei Liu, Yaopeng Liu, Siulai Chan. Direct analysis by an arbitrarily-located-plastic-hinge element: part 2: spatial analysis. J Constr Steel Res 2014;103:316–26.
[25] Tianji Li, Siwei Liu, Siulai Chan. Direct analysis for high-strength steel frames with explicit-model of residual stresses. Eng Struct 2015;100:342–55.
[26] Timoshenko SP. Theory of elastic stability. New York, U. S.: Mc-Graw Hill Book Company; 1936
[27] Gao Y. The calculation and experiment research of three-way gird single layer dome. Master dissertation. China: Tianjin University; 1987.